PROGRESS IN STUDIES OF ENERGY EXTRACTION FROM GEOTHERMAL RESERVOIRS

D.V. Nelson and A. Hunsbedt
Stanford University

THERMAL STRESS FRACTURING STUDY

Analytical studies[1,2] suggest that the thermal stresses produced by fluid circulating in a hot dry rock geothermal reservoir are likely to initiate and propagate cracks in the rock. Such thermally induced cracks will augment the power extracted from a reservoir if they cause a significant increase in effective heat transfer and flow areas. It is thus important to determine experimentally: (a) the conditions under which such cracking will occur, (b) the compatibility of these conditions with expected operating conditions of reservoirs, and (c) the extent to which energy extraction can be enhanced by cracking.

In order to begin a study of items (a) through (c), the behavior of granite samples subjected to thermal stressing is being investigated. In particular, the fracture strength and porosity of the samples is being explored for various combinations of rock temperature and quenching severity. In Murphy's analytical model for thermal stress cracking under full-scale geothermal reservoir conditions,[2] it is hypothesized that cracking will occur in those regions where tensile thermal stress exceeds the "effective" compressive earth stress, assuming that the tensile strength of the rock is negligible. The "effective" compressive stress to be overcome is significantly reduced if the rock is or becomes sufficiently permeable to allow fluid infiltration such that the pore pressure is raised to the hydrostatic level. Also, changes in the porosity of the rock may influence reservoir heat transfer behavior.[3] Thus information on the effect of thermal stressing on strength and porosity will be helpful in improving understanding of both the thermal fracturing and energy extraction characteristics of geothermal reservoirs.

A recently fabricated experimental apparatus used to produce thermal stress is shown schematically in Fig. 1. Granite blocks (5"x5"x10") are slowly heated (less than 2°F/min) to the desired temperature in a well-insulated oven. The blocks are maintained at the prescribed temperature (representative of geothermal hot rock) for several hours to insure uniformity of initial temperature. This uniformity has been confirmed by thermocouple readings at numerous locations inside initial granite samples. To induce thermal stress, the "exposed" face (shown in Fig. 1) is sprayed with water from approximately one hundred small jets. The face is insulated until just before the test to minimize any initial temperature gradients. The quenched face is intended to provide a small-scale simulation of a portion of the face of a hydraulic fracture (without hydrostatic or tectonic stresses acting).

The transient temperature distribution in the granite block can be estimated by treating it as a semi-infinite solid or, equivalently, as a slab of finite thickness with insulated sides. The experimental set-up and block size were designed to make this idealization reasonable. For a constant value of surface heat transfer coefficient, the time-temperature distribution is given by the well-established one-dimensional solution:

$$\frac{T_i - T(z,t)}{T_i - T_\infty} = 1 - \mathrm{erf}\left(\frac{z}{2\sqrt{\alpha t}}\right) - \left[\exp\left(\frac{hz}{k} + \frac{h^2 \alpha t}{k^2}\right)\right] \cdot \left[1 - \mathrm{erf}\left(\frac{z}{2\sqrt{\alpha t}} + \sqrt{\frac{h^2 \alpha t}{k^2}}\right)\right] \qquad (1)$$

where: T = temperature
T_i = initial slab temperature
T_∞ = fluid temperature
h = surface heat transfer coefficient between the fluid and rock
k = rock thermal conductivity
α = rock thermal diffusivity
t = time
z = distance inward from quenched face .

Assuming linear elastic, isotropic, homogeneous behavior, the thermal stresses due to the quenching can be estimated from:

$$\sigma^* = \frac{\sigma(1-\nu)}{E\alpha} = \theta - \frac{2}{b^2}(2b-3z)\int_0^b \theta dz - \frac{6}{b^3}(2z-b)\int_0^b \theta z dz \qquad (2)$$

where: σ^* = nondimensional stress ($\sigma_x = \sigma_y$)
E = rock modulus of elasticity
α = rock coefficient of thermal expansion
ν = rock Poisson's ratio
b = length of block
θ = nondimensional temperature = $\frac{T_i - T(z,t)}{T_i - T_\infty}$.

The time-temperature behavior determined from Eq. 1 is substituted into Eq. 2, and numerical integration performed to obtain σ^*.

Initial tests have been of an exploratory nature, intended to see if significant changes in strength and porosity do result from thermal stressing under representative geothermal conditions. Sierra-white granite

(Raymond, CA Quarry) was used in the tests. Properties of the rock pertinent to the time-temperature and thermal stress analyses are given in Table 1. For the test results considered here, the rock temperature prior to quenching was 450°F. The water temperature was 70°F. For these conditions, the time-temperature distribution along the center-line of several blocks was measured using thermocouples cemented in place at the ends of holes drilled in from the side. Comparison of the measured distributions with those predicted by Eq. 1 indicates a surface heat transfer coefficient during quenching of $h \simeq 300$ Btu/hr-ft^2-°F for the current experimental configuration. The estimated nondimensional thermal stress at various times for this value of h is shown in Fig. 2.

TABLE 1: SIERRA-WHITE GRANITE PROPERTIES

Density, lb/ft^3	ρ	164
Poisson's ratio	ν	0.22
Modulus of elasticity, x10^{-6} psi	E	7.0
Uniaxial tensile strength, psi	σ	1,100
Specific heat, Btu/lb °F	C	0.22
Coefficient of thermal expansion, x10^{-6}/°F	α	4.12
Thermal conductivity, Btu/hr-ft-°F	k	1.57

For the given test conditions, no macrocracking has been observed in those samples tested to date. To investigate the change in strength due to quenching, the blocks were sliced into smaller rectangular specimens (1-1/2"x3"x0.3") and loaded to fracture in three-point bending. (These blocks did not have thermocouple holes.) Based on eight specimens from an unquenched block, the mean elastically-calculated bending stress at fracture was 1,830 psi, with a coefficient of variation of 15%. The bending strength is roughly two-thirds larger than the uniaxial tensile strength. This is to be expected since fracture in bending tends to be governed by an averaged value of stress acting over a volume of material. The bending strength of specimens taken from various positions along the length of a quenched specimen is given in Fig. 3. Also shown in this figure are the strengths of specimens obtained from two blocks, each of which were subjected to five cycles of quenching. There is a significant degradation in strength in those specimens taken from near the quenched face, where tensile thermal stress existed. On the other hand, there is no loss of strength in specimens taken from regions of compressive stress. See Fig. 2. The loss of strength is apparently not due to heating alone (to 450°F); it is likely due to microcracking caused by tensile thermal stress. Although additional tests are needed to better quantify the change in strength, these preliminary results are encouraging in terms of the potential of thermal stress to cause useful fracturing in geothermal reservoirs.

Dye penetrant was applied to one face of some of the specimens after bend testing. Although it was found that this does not provide a satisfactory way of observing microcracking, it was noted that in "unquenched" specimens, the dye either did not seep through to the other side or did so very slowly. In "quenched" specimens, however, the dye penetrated very quickly, indicating a possible increase in permeability.

Currently, the porosity and permeability of thermally-stressed specimens is being determined to see if a significant change occurs. Also, more bend tests of specimens obtained from blocks subjected to various quenching conditions are being conducted. These data will be used in conjunction with existing heat transfer and thermal fracturing models to provide an improved understanding of the role of thermal stress in geothermal reservoir engineering.

HEAT TRANSFER MODEL DEVELOPMENT

A heat transfer model that predicts the water temperature as a function of time at various points in a reservoir when water flows through a rock matrix was developed and reported by Iregui et al.[4] and by Hunsbedt et al.[5] The model is applicable to a fractured rock reservoir produced by the "sweep process" in which high pressure cold water is injected at one point and heated as it flows uniformly to a production point.

Comparison of model predictions and experimental results obtained from the Stanford Geothermal Large Reservoir Model (Chimney Model) showed reasonable agreement at some locations in the reservoir, while significant deviations were found at other locations.[4,5] One reason for the poor agreement was thought to be cross-sectional water temperature differences in the model caused by uneven heating from the vessel steel wall. This effect was not accounted for in the one-dimensional analytic model.

Another experiment of the sweep-type was conducted subsequently for similar experimental conditions, except that the rock matrix porosity was 21% and the permeability was on the order of 30 Darcies, as compared to a 42% porosity and essentially infinite permeability for the earlier experiment. Reduced porosity and permeability for the latter experiment were achieved by filling the voids between the rock segments in the matrix with fine sand (80 to 100 mesh). A comparison of measured and predicted water temperatures for this experiment was also performed, and results are presented in the following.

A summary of the input parameters to the sweep heat transfer model for the present experimental conditions is given in Table 2. The effective rock radius for the rock/sand system was calculated to be 0.105 ft using the technique presented in refs. 4 and 5. A very significant parameter listed in Table 2 is the number of heat transfer units parameter, N_{tu}. It is the ratio between the water residence time and the rock time constant, and calculated to be 44.8 in this case. This is a relatively large value, indicating that the reservoir is not heat transfer limited. Previous studies reported in ref. 4 showed that a reservoir is heat transfer limited when $N_{tu} \lesssim 10$. In that case, the heat transfer rate from the rock is not sufficient to heat the water, resulting in an early water temperature drop and ineffective energy extraction from the rock.

TABLE 2: SUMMARY OF INPUT PARAMETERS TO THE SWEEP HEAT TRANSFER MODEL

EXPERIMENTAL CONDITIONS	
Initial reservoir temperature	460°F
Recharge water temperature	60°F
Production time	4.5 hr
Production/recharge rate	198 lb/hr
RESERVOIR CONDITIONS	
Porosity	0.21
Cross-sectional area	3.27 ft^2
Length	5.08 ft
Effective rock radius	0.105 ft
External heat transfer	1,811 Btu/ft
DERIVED PARAMETERS	
Modified storage ratio	0.23
Superficial flow velocity	1.03 ft/hr
Pore flow velocity	4.92 ft/hr
water residence time	1.03 hr
Rock Biot number	22.5
Effective time constant	0.023 hr
Number of transfer units	44.8
Normalized external heat transfer	0.026

The predicted water temperature at various elevations is compared in Fig. 4 to measured temperatures at points where such measurements were made in the experimental system. (Note that $x^* = 0$ is at the cold water injection point.) The following observations are made relative to Fig. 4:

1. Predicted water temperatures do not drop off as fast as do the measured temperatures initially.

2. At later times in the cooldown process, predicted water temperature curves drop below the measured ones and remain generally lower.

3. Exceptions to the above occur at the top ($x^* = 0.88$ and 0.97) where the predicted temperature is always higher than the measured value.

Reasons for discrepancies between predicted and measured water temperatures include a 50°F cross-sectional temperature mal-distribution measured near the top of the reservoir when such instrumentation was available. (Temperature measurements given in Fig. 4 were obtained along the rock matrix center line.) The one-dimensional analysis does not account for such two-dimensional effects.

Attempts to improve model predictions were made. For example, improved predictions were achieved when a value of N_{tu} = 5.0 was used rather than the theoretical value of 44.8. These predictions are seen in Fig. 4 to be considerably better than before, particularly near the middle elevation of the reservoir (x* = 0.5). In addition, the slope of the curves are in much better agreement.

The results indicate that more work is needed to determine the causes of the discrepancy between model predictions and experimental data. An effort is currently underway to determine if a computational error is involved in the numerical inversion routine used to obtain the solution. Numerical integration of the partial differential equations will be used for comparison. Further energy extraction experiments will be conducted after the analytical model problem has been resolved.

REFERENCES

1. Nemat-Nasser, S., and Ohtsubo, H.: "Fluid Flow and Heat Transfer Through Hydraulically Induced Fractures in Hot, Dry Rock Masses," J. Pressure Vessel Tech., Trans. ASME (Aug. 1978), 100, 277.

2. Murphy, H.D.: "Thermal Stress Cracking and the Enhancement of Heat Extraction from Fractured Geothermal Reservoirs," Report LA-7235-MS, Los Alamos Scientific Laboratory (Apr. 1978).

3. Hunsbedt, A., Kruger, P., and London, A.L.: "Energy Extraction from a Laboratory Model Fractured Geothermal Reservoir," J. Pet. Tech. (May 1978), 712-718.

4. Iregui, R., Hunsbedt, A., Kruger, P., and London, A.L.: "Analysis of Heat Transfer and Energy Recovery in Fractured Geothermal Reservoirs," Report SGP-TR-31, Stanford Geothermal Program (June 1978).

5. Hunsbedt, A., Iregui, R., Kruger, P., and London, A.L.: "Energy Recovery from Fracture-Simulated Geothermal Reservoirs," paper for the 18th ASME-AIChE National Heat Transfer Conference.

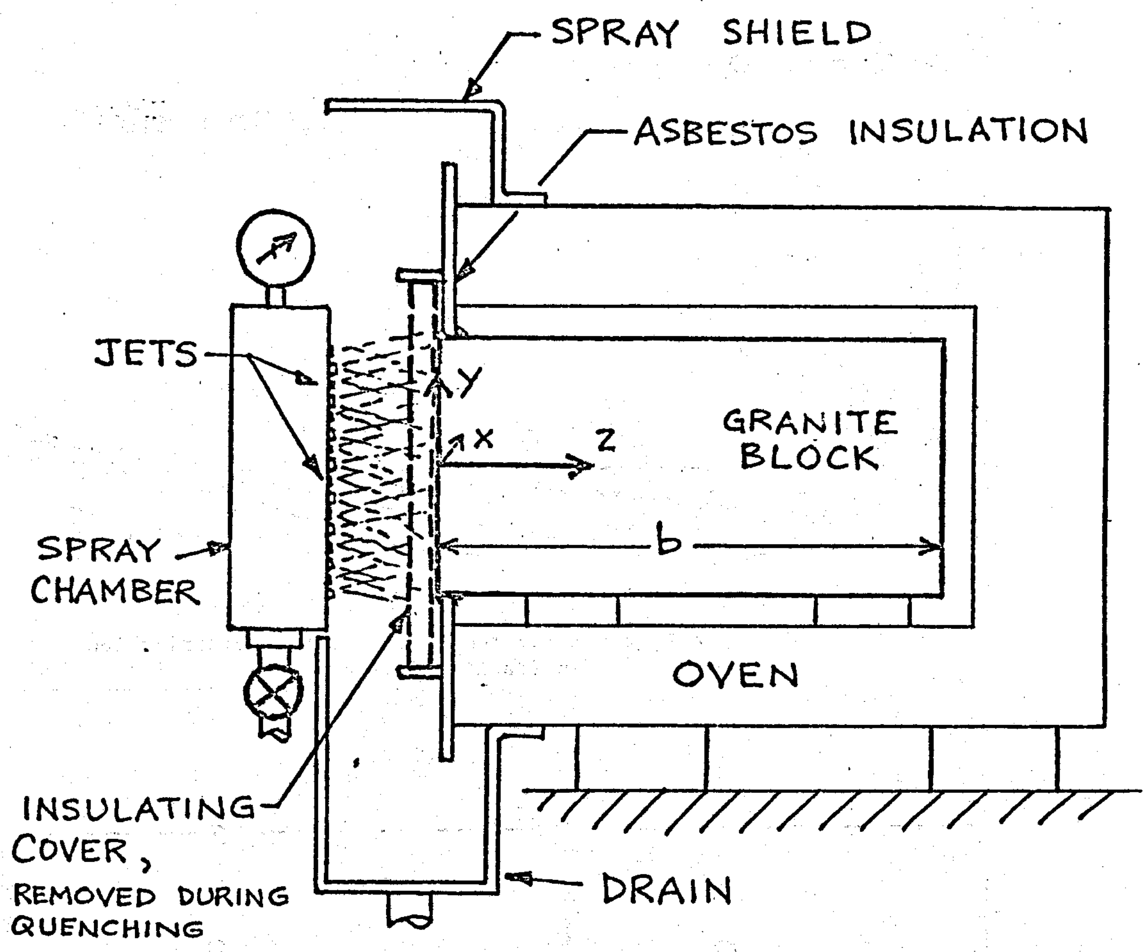

Fig. 1 - Schematic of Thermal Stress Fracturing Experimental Apparatus

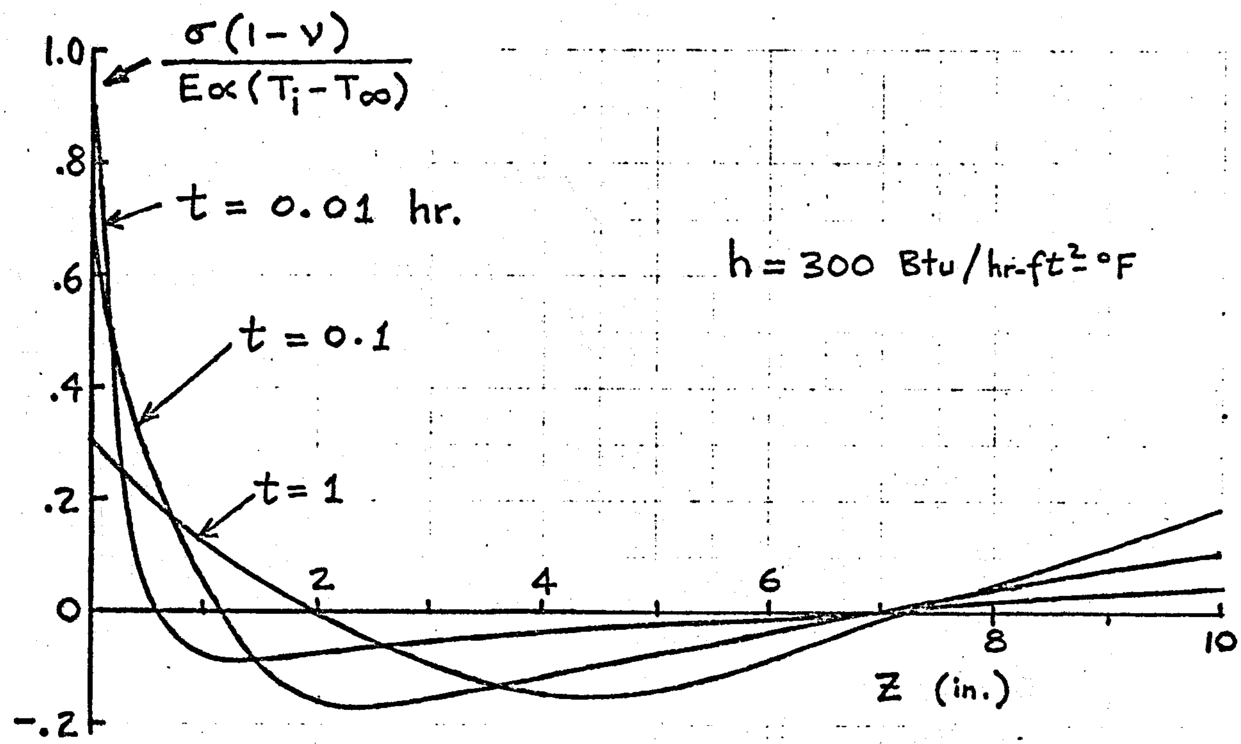

Fig. 2 - Estimated Thermal Stress Distribution in Granite Block

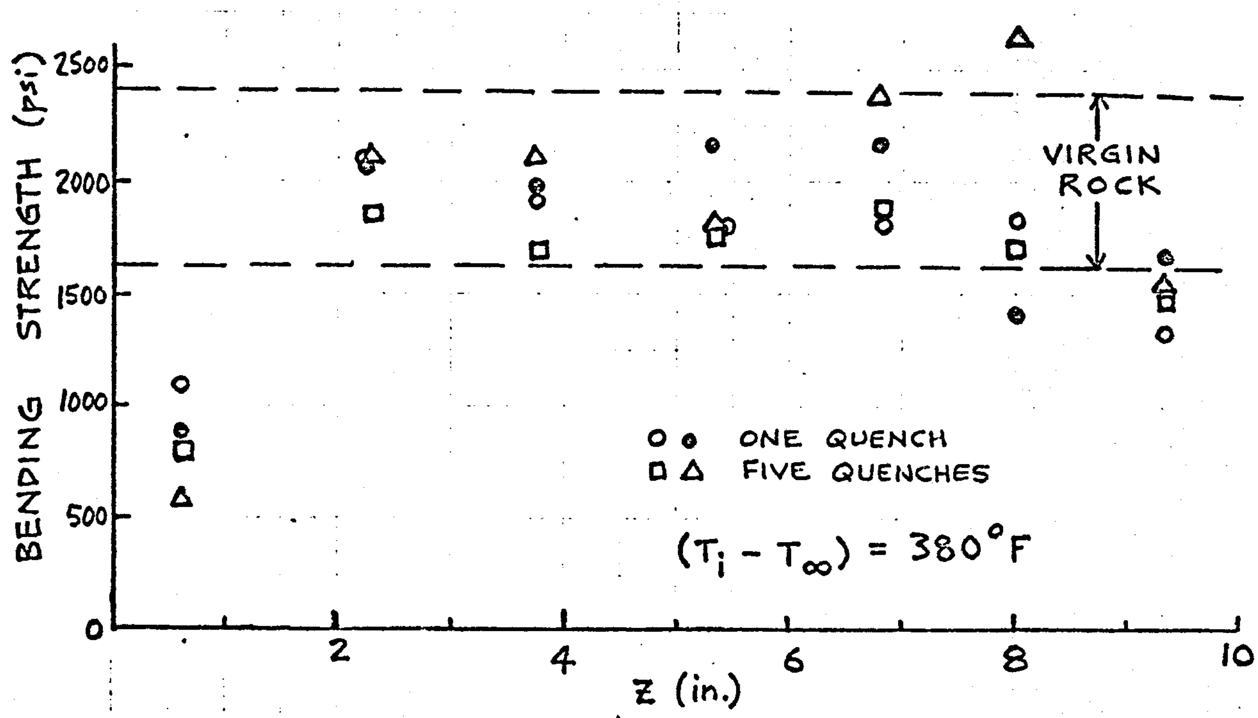

Fig. 3 - Bending Strength of Specimens Taken from Block

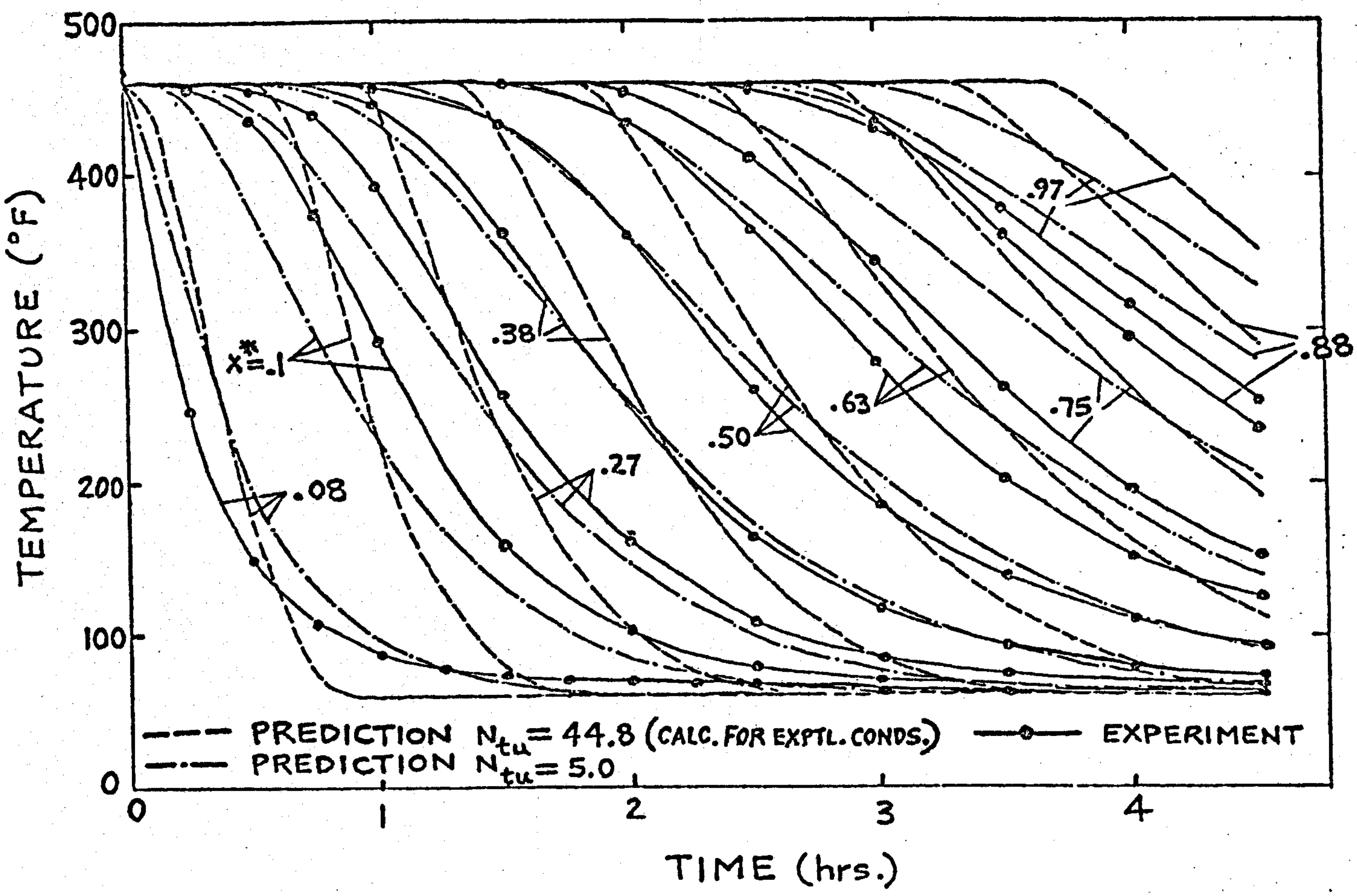

Fig. 4 - Comparison of Experimental and Predicted Water Temperatures